

# Towards dual light control of a catalytically-driven chemical reaction cycle

Jorge S. Valera<sup>1,2\*</sup>, Álvaro López-Acosta<sup>1</sup> and Thomas M. Hermans<sup>1,2\*</sup>

<sup>1</sup>IMDEA Nanociencia, C/ Faraday 9, 28049 Madrid, Spain

<sup>2</sup>Université de Strasbourg, CNRS, UMR7140, 4 Rue Blaise Pascal, 67081 Strasbourg, France

\*jorge.santos@imdea.org & thomas.hermans@imdea.org

**KEYWORDS** Dissipative self-assembly - out-of-equilibrium - chemical reaction cycles - photoredox catalysis - chemical fuels

**Abstract:** Chemically-fueled chemical reaction networks (CRNs) are key in controlling dissipative self-assembly. Having catalysts gating fuel consumption for both the activation and deactivation chemistry of (assembly-prone) monomers and controlling the catalytic activity with an external stimulus would provide better control over where, when, and how long self-assembled structures can form. Here we achieve light control over monomer activation and subsequent assembly into supramolecular fibers, and partial light control over deactivation and fiber disassembly. Activation proceeds via photoredox catalysis under visible light, whereas deactivation is achieved by organometallic catalysis that relies on a photocaged pre-fuel activated by ultraviolet light. Overall, we show how supramolecular fibers can be formed by visible light and how their destruction is accelerated by ultraviolet light.

Living cells rely on enzymatic chemical reaction networks (CRNs) to regulate the self-assembly of supramolecular structures like actin filaments and microtubules.<sup>1-5</sup> The latter are responsible for biological processes like the formation of the mitotic spindle,<sup>6,7</sup> whereas the former play a key role in cell motility.<sup>8-10</sup> Inspired by nature, an increasing number of artificial CRNs have been used to control self-assembly processes in the last decade.<sup>11-13</sup> Many of those CRNs<sup>14,15</sup> involve the consumption of a reagent or substrate (termed ‘activating fuel’) to activate a monomer prone to self-assemble. Subsequently, the monomer is deactivated by solvent hydrolysis,<sup>16,17</sup> due to same type of chemistry as used in activation (like thiol-ester<sup>18</sup> or thiol-disulfide<sup>19</sup> exchange), or by other means like redox chemistry or Michael additions.<sup>20-22</sup> So far, catalysis in artificial CRNs to control self-assembly has been achieved by enzymes,<sup>23-25</sup> transition metal catalysis<sup>26,27</sup> and organocatalysis<sup>28,29</sup>, and its benefits have been discussed recently.<sup>30</sup> Especially appealing is the ability to turn on the catalyst on demand or to modulate the catalysts activity in situ. In addition, having catalytic control over the CRN permits the storage of (excess) fuels in the system until a signal or a stimulus is provided.<sup>31</sup> Light is a perfect tool to this end, and to date has been used in the form of photoisomerization<sup>32-34</sup>, photoreduction,<sup>35</sup> photocage molecules<sup>36</sup>, or photo-switchable molecular motors.<sup>37</sup> However, full catalytic control in a chemically fueled CRN using different wavelengths has not been achieved. Here we show a CRN that uses photoredox catalysis (**Cat1** in Figure 1) to convert monomer SachOL—to form (activated monomer) SachCHO that assembles into supramolecular fibers—and transition metal catalysis (**Cat2**) to deactivate SachCHO back to SachOL. Photocage fuel “PC-Formate” absorbs at a different wavelength than **Cat1**, therefore activation and (partially) deactivation can be controlled independently and on demand.

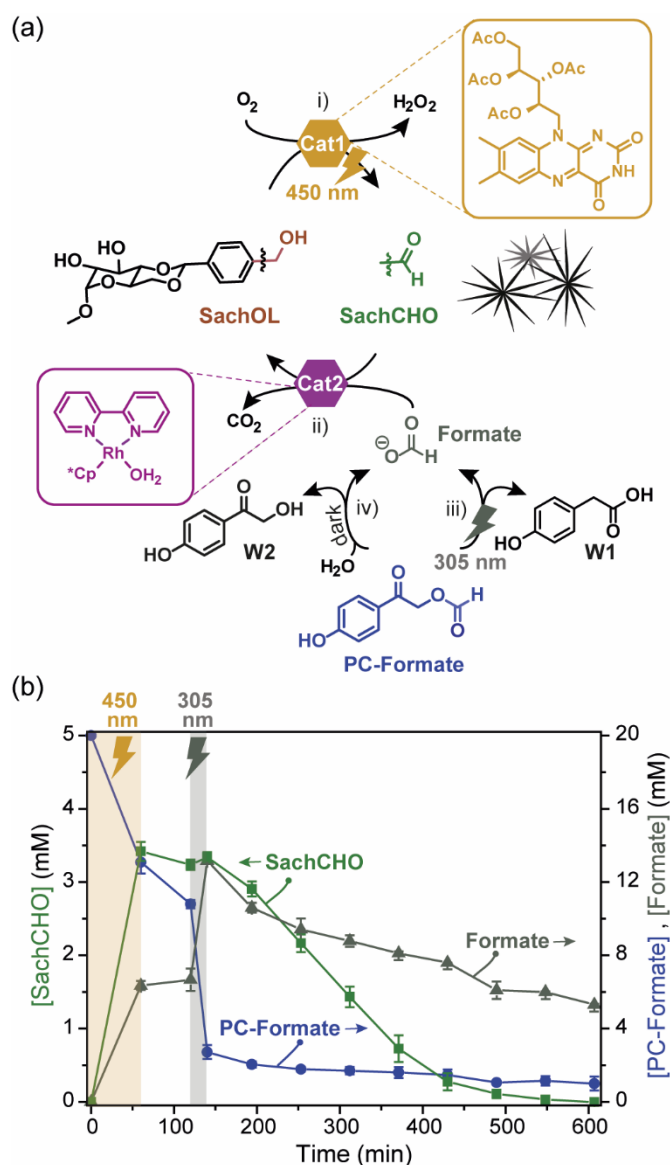


**Figure 1.** (a) Towards dual wavelength control over a catalytically-driven CRN, forming transient SachCHO fibers. Oxidation of SachOL to SachCHO by using riboflavin tetraacetate (RFTA, **Cat1**) by 450 nm irradiation. Reduction of SachCHO to SachOL by [Cp\*Rh(Bpy)(H)]<sup>+</sup>, which is generated from [Cp\*Rh(Bpy)(H<sub>2</sub>O)]<sup>2+</sup> (**Cat2**) using formate as hydride source. Photocleavage of *p*-hydroxyphenacyl formate (**PC-Formate**), releases formate with 305 nm light producing *p*-hydroxyphenylacetic acid (W1) as main by-product. PC-Formate also releases the fuel in the dark at longer times upon hydrolysis, producing *α*-hydroxyketone (W2) as by-product. Steps i-iv are described in the main text. (b) Relative species concentration by <sup>1</sup>H NMR. [SachOL]<sub>0</sub> = 5 mM, [RFTA]<sub>0</sub> = 1 mM, [[Cp\*Rh(Bpy)(H<sub>2</sub>O)]<sup>2+</sup>]<sub>0</sub> = 1 mM, [PC-Formate]<sub>0</sub> = 20 mM in THF-d<sub>8</sub>/0.5 M Phosphate buffer pH = 6 1/9 mixtures. Yellow/orange shade and orange lightning bolt denote irradiation with 450 nm and grey shade and lightning bolt with 305 nm. Error bars are standard deviations over duplicate experiments.

We have previously reported chemically fueled gel-sol-gel<sup>38,39</sup> and sol-gel-sol-gel-sol transitions<sup>40</sup> using saccharide-based benzaldehyde derivative SachCHO. In the latter examples we converted the aldehyde of SachCHO to the hydroxy-sulfonate<sup>38,39</sup> or thiazinane<sup>40</sup> analogs that are negatively charged and therefore disassembled in aqueous solution. In the current work, we convert SachCHO to alcohol analog SachOL (see Section 2 in Supporting Information for synthetic details and characterization) which forms crystalline needles in water (see Fig. S1). However, fiber formation of SachOL is precluded in THF/0.5 M phosphate buffer mixtures (1/9 ratio, pH=6) at the concentrations used in the remainder of the paper whereas SachCHO maintains its ability to form thin, long fibers sprouting from aster-like structures at 7-8 mM (see Fig. S2).

The selective oxidation of benzylic alcohol SachOL to aldehyde SachCHO is achieved by riboflavin tetraacetate (RFTA, **Cat1** in Fig. 1a) as photocatalyst upon 450 nm irradiation,<sup>41-43</sup> in high yields after 90 mins as shown by <sup>1</sup>H NMR experiments (Fig. S3). RFTA is reduced while oxidizing the benzyl alcohol and is then regenerated by oxygen (*i.e.* the activating fuel), producing H<sub>2</sub>O<sub>2</sub> as waste (step *i* in Fig.1a). This reaction is first order in SachOL (Fig. S4-S5) showing an estimated half-time  $t_{1/2} = 68$  min with 20% **Cat 1** loads (Table S1). The (deactivating) reduction of SachCHO to SachOL is quantitative through catalytic hydride transfer by [Cp\*Rh(Bpy)(H)]<sup>+</sup>, which is generated *in situ* from the pre-catalyst [Cp\*Rh(Bpy)(H<sub>2</sub>O)]<sup>2+</sup> (**Cat2** in Fig. 1a, step *ii*) and formate as hydride source to produce CO<sub>2</sub> as waste (Fig. S6). This reaction is zeroth order in SachCHO and first order in formate in the current conditions, indicating a more complex behavior in the case of **Cat2** which is out of the scope of this paper (see the section 'Kinetic Analysis Discussion' in SI and Fig. S7-S8 and Tables S2-S3 for the estimated  $t_{1/2}$  of SachCHO at different conditions).<sup>44</sup> To control the deactivation by light, we photo-uncage formate from *p*-hydroxyphenacyl formate (PC-Formate in Fig. 1, step *iii*) at 305 nm, where it preferentially absorbs in comparison with RFTA (compare  $\lambda = 305$  nm for PC-Formate versus  $\lambda = 450$  nm for RFTA in Fig. S9).<sup>45</sup> The photo uncaging of formate happens in less than 10 minutes in an isolated experiment (Fig. S10), producing *p*-hydroxyphenylacetic acid side product (W1 in Fig. 1a).<sup>45</sup> In the complete cycle (as in Fig. 1a) both RFTA and PC-Formate absorb (*i.e.*, they compete for the same photons), and hence the time to release formate is approximately 40% slower (Fig. S10).

We explored different **Cat2** loading for deactivation upon photo uncaging of formate, to achieve full conversion to SachOL after 400 min (see 20% **Cat2** in Fig. S11 and Table S4 for the estimated  $t_{1/2} = 192$  min).<sup>46</sup> These results indicate that activation proceeds quicker than deactivation in the conditions employed in the cycle. PC-Formate itself hydrolyses to the  $\alpha$ -hydroxyketone (W2, step *iv* in Fig. 1a) following a pseudo first order reaction in dark conditions, although slow enough to store the photocaged fuel for suitable times ( $k_{\text{exp}} = 1.65 \pm 0.03 \times 10^{-3} \text{ min}^{-1}$  and  $t_{1/2} = 420$  min) in absence of irradiation (Fig. S12-S13).<sup>45</sup>

Combining **Cat1**, **Cat2**, and PC-Formate into the full CRN, we can transiently form SachCHO by irradiation of activating 450 nm and deactivating 305 nm light as can be seen by <sup>1</sup>H NMR (Figure 1b and 2a). We obtained ~50% and ~70 % peak activation of SachOL to SachCHO after 30 min or 60 mins of irradiation, respectively (cf. Figure 2b, upper or lower panel). Further irradiation with  $\lambda = 305$  nm releases formate from the photocage, accelerating the deactivation of SachCHO to SachOL.

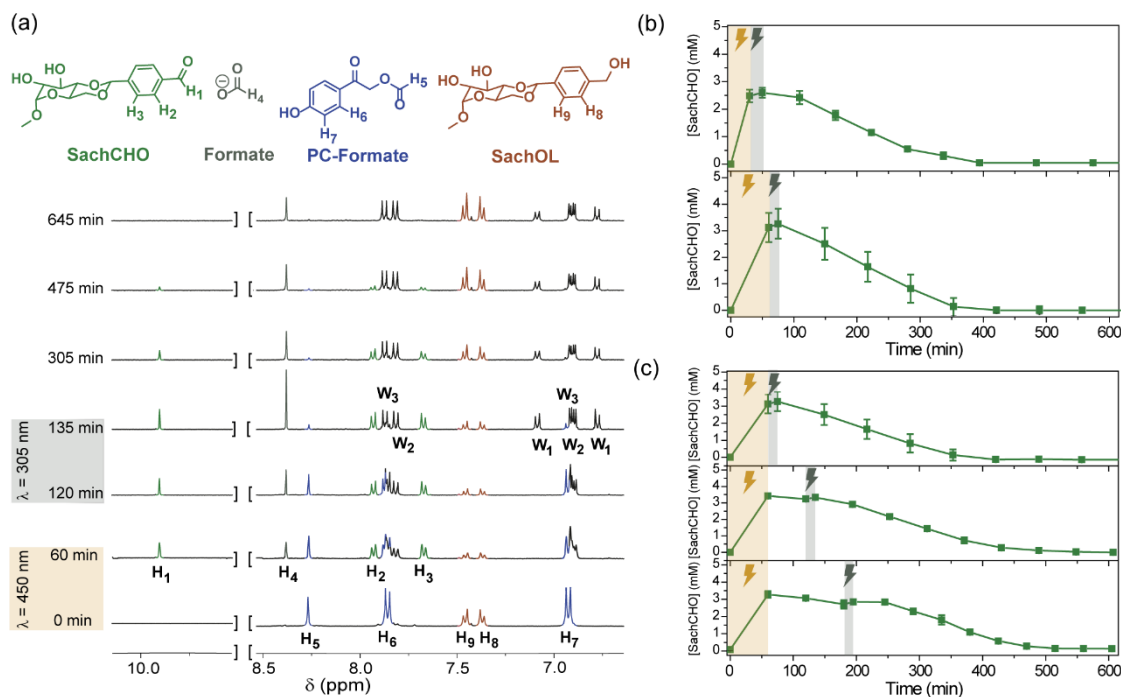


**Figure 2.** (a) <sup>1</sup>H NMR spectra of the cycle at different times. [SachOL]<sub>0</sub> = 5 mM, [RFTA]<sub>0</sub> = 1 mM, [[Cp\*Rh(Bpy)(H<sub>2</sub>O)]<sup>2+</sup>]<sub>0</sub> = 1 mM, [PC-Formate]<sub>0</sub> = 20 mM in THF-d<sub>8</sub>/0.5 M Phosphate buffer pH=6 1/9 mixtures. (b) Effect of time of activation irradiation in SachCHO conversion. Upper panel denotes 30 min of 450 nm irradiation and lower panel 60 min of 450 nm irradiation, followed by immediate irradiation with 305 nm during 15 min in both cases. (c) Modulation of the lifetime of SachCHO by spacing the time between irradiation 450 nm during 60 min and delaying irradiation 305 nm (applied during 15 min) for 0h (upper panel), 1h (middle panel) and 2h (lower panel). Yellow/orange shade and orange lightning bolt denote irradiation with 450 nm and grey shade and lightning bolt with 305 nm. Error bars are standard deviations over duplicate experiments.

Nevertheless, the photocontrol over deactivation was limited by the stability of PC-Formate in the cycle (See section “PC-formate stability in the dark...” on p. 11 of the Supporting Information). These undesired interactions are a typical limitation in the development of CRNs.<sup>47</sup> We noticed an increase in formate release from PC-Formate in the dark with all the components of the cycle (Fig. S14-S15,  $k_{\text{exp}} = 4.1 \pm 0.1 \times 10^{-3} \text{ min}^{-1}$  and  $t_{1/2} = 171 \text{ min}$ ) and to a greater extent upon 450 nm irradiation in these conditions (Fig. S16-S19, with an estimated  $t_{1/2} = 90 \text{ min}$ ). This latter interaction also generates the *p*-hydroxyacetophenone (W3) under 450 nm irradiation (Fig. 2a and Fig. S20 for the complete NMR spectra of the cycle). We hypothesize that this enhanced release arises from the interaction of RFTA and the RFTA semiquinone radicals with PC-Formate, respectively, in a similar way that has been reported for other radical species<sup>48</sup> (see Scheme S1 for a detailed description of the complete CRN, plausible interactions and all the species involved in each pathway). Although this undesired reactivity leads to the release of ~30% of formate (1.3 eq. in the conditions utilized) after 60 min of irradiation, we can still store enough pre-fuel PC-Formate in our system to partially exert photocontrol over the backward reaction, attaining ~1.8 acceleration when compared to the deactivation without light (Fig. S17-18, note that the remaining PC-Formate without deactivating 305 nm light is at least 2x times the one observed with irradiation, which explains this enhancement in agreement with Fig. S8 and Table S3).

Still, this approach enables us to modulate the lifetime of the transient species with the same amounts of fuels and catalysts by spacing the time between irradiations (Fig. 2c). After irradiation during 60 min with 450 nm, we can then delay the triggering of the deactivation for 0h (Fig. 2c, upper panel), 1h (Fig. 2c, middle panel) and 2h (Fig. 2c, lower panel), extending in this way the lifetime of SachCHO under the same conditions and concentrations of components of the cycle (notice that the estimated SachCHO half-time increases from  $t_{1/2} = 250 \text{ min}$  to 315 min, and to 360 min, respectively).

At longer activation irradiation time (90 min), sufficient formate is released simultaneously to not require further deactivating 305 nm light (Fig. S19). We observed 90% SachOL→SachCHO conversion, which fully reverts to SachOL in 10 h since more than 50% of formate (2 eq.) had been simultaneously released by photo-uncaging and the rest of the PC-formate hydrolyzes with time. **That is, a full assembly-disassembly cycle is feasible upon just 450 nm irradiation.**

**Reverting back to both light activation and deactivation, the full** CRN was followed by bright field microscopy (Figure 3, Video 1 and Fig. S21 for comparable <sup>1</sup>H NMR experiments). For these experiments we increased the concentration of SachOL from 5 mM to 10 mM and reduced [Cp\*Rh(Bpy)(H<sub>2</sub>O)]<sup>2+</sup> load to 15% to **obtain sufficiently large SachCHO fibers for optical microscopy, as well as to exert** photocontrol over the deactivation reaction (note the critical gel concentration of SachCHO is 21 mM for heating/cooling,<sup>39</sup> but at lower concentrations fibers still form).

A solution of SachOL, **Cat1**, **Cat2** and PC-Formate is subjected to irradiation with  $\lambda = 450$  nm during 75 min, converting around 80% of SachOL to SachCHO (Fig. 3a-3b and Fig. S21), **the minimum conversion needed to see the formation of fibers in these conditions.** At this time, nucleation and growth of asters-like structures characteristic of SachCHO takes place during the next 55 min (Fig. 3c-3h). Subsequent irradiation with  $\lambda = 305$  nm during 15 min releases the remaining formate (Fig. 3i and Fig. S21). **As can be seen in Fig. S21 by comparing the green and black lines, although deactivation of SachCHO in solution starts after formate release, the complete removal of SachCHO fibers takes more time (i.e., there is a shielding effect), starting at 840 min and being completely removed after 1110 min (Fig. 3j-3o and Fig. S21).**

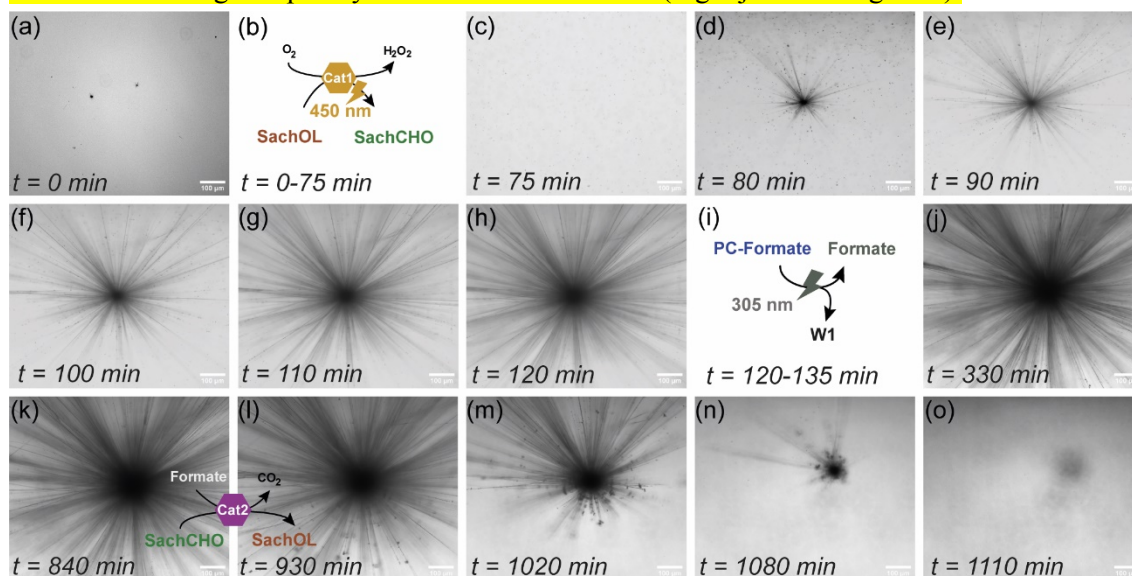


**Figure 3.** Bright field microscopy images of the light controlled, catalytically driven-CRN at different stages: (a) **A solution of SachOL, Cat1, Cat2 and PC-Formate,** (b) irradiation with 450 nm activating light for 75 min to convert SachOL in SachCHO, (c-h) nucleation and elongation of SachCHO fibers into aster-like structures during the next 55 min, (i) irradiation with deactivation 305 nm light releases formate from PC-Formate, (j-o) deactivation of SachCHO ensues followed by visible shrinking of its fibers at 700 min and complete disappearance due to its conversion to SachOL. [SachOL]<sub>0</sub> = 10 mM, **Cat1** = [RFTA]<sub>0</sub> = 1.5 mM, **Cat2** = [[Cp\*Rh(Bpy)(H<sub>2</sub>O)]<sup>2+</sup>]<sub>0</sub> = 1.5 mM, [PC-Formate]<sub>0</sub> = 30 mM in THF-d<sub>8</sub>/0.5 M Phosphate buffer pH=6 1/9 mixtures. All scale bars are 100  $\mu$ m. See also Supporting Video 1.

Overall, we have shown **our efforts towards a** dual light controlled CRN to achieve activation/assembly by photoredox catalysis and deactivation/disassembly by transition metal catalysis combined with a photocaged fuel. **We can fully control the onset of transient supramolecular fibers and partially, their life-time by using two different wavelengths of light that each control a distinct catalytic system.** Our approach constitutes a first step towards full photocatalytic control in fuel-driven self-assembly, with control over the lifetime of the transient species at the same catalyst loading and with an abundant storage of (pre-)fuels in the system until needed or to sustain long-lived non-equilibrium steady states. Future systems with more stable

(photocaged) pre-fuels would be desirable to further extend the usable time-window of catalytic CRNs. Spatiotemporal control over forming and destroying supramolecular fibers could be a basis for  $\mu\text{m}$ -sized soft robots.<sup>49,50</sup>

### Acknowledgments

J.S.V. and T.M.H. acknowledge funding from ERC-2017-STG “Life-Cycle” (757910). A.L-A. acknowledges the European Union’s Horizon 2020 Research and Innovation Program under the Marie Skłodowska-Curie grant agreement no. 812868 for Ph.D. funding. We thank Marten L. Ploeger and Alex Blokhuis for fruitful discussions.

### Conflict of interest

There are no conflicts to declare.

### References

- (1) Wong, A. S. Y.; Huck, W. T. S. Grip on Complexity in Chemical Reaction Networks. *Beilstein Journal of Organic Chemistry* **2017**, *13*, 1486–1497. <https://doi.org/10.3762/bjoc.13.147>.
- (2) Rottner, K.; Faix, J.; Bogdan, S.; Linder, S.; Kerkhoff, E. Actin Assembly Mechanisms at a Glance. *Journal of Cell Science* **2017**, *130* (20), 3427–3435. <https://doi.org/10.1242/jcs.206433>.
- (3) Mandelkow, E. M.; Mandelkow, E.; Milligan, R. A. Microtubule Dynamics and Microtubule Caps: A Time-Resolved Cryo-Electron Microscopy Study. *Journal of Cell Biology* **1991**, *114* (5), 977–991. <https://doi.org/10.1083/jcb.114.5.977>.
- (4) Conde, C.; Cáceres, A. Microtubule Assembly, Organization and Dynamics in Axons and Dendrites. *Nature Reviews Neuroscience* **2009**, *10* (5), 319–332. <https://doi.org/10.1038/nrn2631>.
- (5) Fletcher, D. A.; Mullins, R. D. Cell Mechanics and the Cytoskeleton. *Nature* **2010**, *463* (7280), 485–492. <https://doi.org/10.1038/nature08908>.
- (6) Bastiaens, P.; Caudron, M.; Niethammer, P.; Karsenti, E. Gradients in the Self-Organization of the Mitotic Spindle. *Trends in Cell Biology* **2006**, *16* (3), 125–134. <https://doi.org/10.1016/j.tcb.2006.01.005>.
- (7) Prosser, S. L.; Pelletier, L. Mitotic Spindle Assembly in Animal Cells: A Fine Balancing Act. *Nature Reviews Molecular Cell Biology* **2017**, *18* (3), 187–201. <https://doi.org/10.1038/nrm.2016.162>.
- (8) Mitchison, T. J.; Cramer, L. P. Actin-Based Cell Motility and Cell Locomotion. *Cell* **1996**, *84* (3), 371–379. [https://doi.org/10.1016/S0092-8674\(00\)81281-7](https://doi.org/10.1016/S0092-8674(00)81281-7).
- (9) Pollard, T. D.; Borisy, G. G. Cellular Motility Driven by Assembly and Disassembly of Actin Filaments. *Cell* **2003**, *112* (4), 453–465. [https://doi.org/10.1016/S0092-8674\(03\)00120-X](https://doi.org/10.1016/S0092-8674(03)00120-X).
- (10) Blanchoin, L.; Boujemaa-Paterski, R.; Sykes, C.; Plastino, J. Actin Dynamics, Architecture, and Mechanics in Cell Motility. *Physiological Reviews* **2014**, *94* (1), 235–263. <https://doi.org/10.1152/physrev.00018.2013>.
- (11) Van Rossum, S. A. P.; Tena-Solsona, M.; Van Esch, J. H.; Eelkema, R.; Boekhoven, J. Dissipative Out-of-Equilibrium Assembly of Man-Made Supramolecular Materials. *Chemical Society Reviews* **2017**, *46* (18), 5519–5535. <https://doi.org/10.1039/c7cs00246g>.
- (12) Weißenfels, M.; Gemen, J.; Klajn, R. Dissipative Self-Assembly: Fueling with Chemicals versus Light. *Chem* **2021**, *7* (1), 23–37. <https://doi.org/10.1016/j.chempr.2020.11.025>.
- (13) Sharko, A.; Livitz, D.; De Piccoli, S.; Bishop, K. J. M.; Hermans, T. M. Insights into Chemically Fueled Supramolecular Polymers. *Chem. Rev.* **2022**, *122* (13), 11759–11777. <https://doi.org/10.1021/acs.chemrev.1c00958>.
- (14) Singh, N.; Formon, G. J. M.; De Piccoli, S.; Hermans, T. M. Devising Synthetic Reaction Cycles for Dissipative Nonequilibrium Self-Assembly. *Advanced Materials* **2020**, *32* (20), 1–6. <https://doi.org/10.1002/adma.201906834>.

- (15) Rieß, B.; Grötsch, R. K.; Boekhoven, J. The Design of Dissipative Molecular Assemblies Driven by Chemical Reaction Cycles. *Chem* **2020**, *6* (3), 552–578. <https://doi.org/10.1016/j.chempr.2019.11.008>.
- (16) Boekhoven, J.; Brizard, A. M.; Kowlgi, K. N. K.; Koper, G. J. M.; Eelkema, R.; Van Esch, J. H. Dissipative Self-Assembly of a Molecular Gelator by Using a Chemical Fuel. *Angewandte Chemie - International Edition* **2010**, *49* (28), 4825–4828. <https://doi.org/10.1002/anie.201001511>.
- (17) Tena-Solsona, M.; Rieß, B.; Grötsch, R. K.; Löhrer, F. C.; Wanzke, C.; Käs Dorf, B.; Bausch, A. R.; Müller-Buschbaum, P.; Lieleg, O.; Boekhoven, J. Non-Equilibrium Dissipative Supramolecular Materials with a Tunable Lifetime. *Nature Communications* **2017**, *8* (May), 1–8. <https://doi.org/10.1038/ncomms15895>.
- (18) Dambeniaks, A. K.; Vu, P. H. Q.; Fyles, T. M. Dissipative Assembly of a Membrane Transport System. *Chem. Sci.* **2014**, *5* (9), 3396–3403. <https://doi.org/10.1039/C4SC01258E>.
- (19) Morrow, S. M.; Colomer, I.; Fletcher, S. P. A Chemically Fuelled Self-Replicator. *Nature Communications* **2019**, *10* (1), 1011. <https://doi.org/10.1038/s41467-019-08885-9>.
- (20) Leira-Iglesias, J.; Tassoni, A.; Adachi, T.; Stich, M.; Hermans, T. M. Oscillations, Travelling Fronts and Patterns in a Supramolecular System. *Nature Nanotechnology* **2018**, *13* (11), 1021–1027. <https://doi.org/10.1038/s41565-018-0270-4>.
- (21) Klemm, B.; Lewis, R. W.; Piergentili, I.; Eelkema, R. Temporally Programmed Polymer – Solvent Interactions Using a Chemical Reaction Network. *Nature Communications* **2022**, *13* (1), 6242. <https://doi.org/10.1038/s41467-022-33810-y>.
- (22) Sharko, A.; Spitzbarth, B.; Hermans, T. M.; Eelkema, R. Redox-Controlled Shunts in a Synthetic Chemical Reaction Cycle. *J. Am. Chem. Soc.* **2023**, *145* (17), 9672–9678. <https://doi.org/10.1021/jacs.3c00985>.
- (23) Debnath, S.; Roy, S.; Ulijn, R. V. Peptide Nanofibers with Dynamic Instability through Nonequilibrium Biocatalytic Assembly. *Journal of the American Chemical Society* **2013**, *135* (45), 16789–16792. <https://doi.org/10.1021/ja4086353>.
- (24) Dhiman, S.; Jain, A.; Kumar, M.; George, S. J. Adenosine-Phosphate-Fueled, Temporally Programmed Supramolecular Polymers with Multiple Transient States. *Journal of the American Chemical Society* **2017**, *139* (46), 16568–16575. <https://doi.org/10.1021/jacs.7b07469>.
- (25) Sorrenti, A.; Leira-Iglesias, J.; Sato, A.; Hermans, T. M. Non-Equilibrium Steady States in Supramolecular Polymerization. *Nature Communications* **2017**, *8* (May), 1–8. <https://doi.org/10.1038/ncomms15899>.
- (26) Wood, C. S.; Browne, C.; Wood, D. M.; Nitschke, J. R. Fuel-Controlled Reassembly of Metal–Organic Architectures. *ACS Cent. Sci.* **2015**, *1* (9), 504–509. <https://doi.org/10.1021/acscentsci.5b00279>.
- (27) Colomer, I.; Morrow, S. M.; Fletcher, S. P. A Transient Self-Assembling Self-Replicator. *Nature Communications* **2018**, *9* (1), 2239. <https://doi.org/10.1038/s41467-018-04670-2>.
- (28) Bal, S.; Das, K.; Ahmed, S.; Das, D. Chemically Fueled Dissipative Self-Assembly That Exploits Cooperative Catalysis. *Angewandte Chemie International Edition* **2019**, *58* (1), 244–247. <https://doi.org/10.1002/anie.201811749>.
- (29) van der Helm, M. P.; Wang, C.-L.; Fan, B.; Macchione, M.; Mendes, E.; Eelkema, R. Organocatalytic Control over a Fuel-Driven Transient-Esterification Network\*\*. *Angewandte Chemie International Edition* **2020**, *59* (46), 20604–20611. <https://doi.org/10.1002/anie.202008921>.
- (30) van der Helm, M. P.; de Beun, T.; Eelkema, R. On the Use of Catalysis to Bias Reaction Pathways in Out-of-Equilibrium Systems. *Chem. Sci.* **2021**, *12* (12), 4484–4493. <https://doi.org/10.1039/D0SC06406H>.
- (31) van der Helm, M. P.; Li, G.; Hartono, M.; Eelkema, R. Transient Host–Guest Complexation To Control Catalytic Activity. *J. Am. Chem. Soc.* **2022**, *144* (21), 9465–9471. <https://doi.org/10.1021/jacs.2c02695>.
- (32) Kundu, P. K.; Samanta, D.; Leizrowice, R.; Margulis, B.; Zhao, H.; Börner, M.; Udayabhaskararao, T.; Manna, D.; Klajn, R. Light-Controlled Self-Assembly of Non-

- Photoresponsive Nanoparticles. *Nature Chemistry* **2015**, *7* (8), 646–652. <https://doi.org/10.1038/nchem.2303>.
- (33) Chen, R.; Neri, S.; Prins, L. J. Enhanced Catalytic Activity under Non-Equilibrium Conditions. *Nature Nanotechnology* **2020**, *15* (10), 868–874. <https://doi.org/10.1038/s41565-020-0734-1>.
- (34) Nakamura, K.; Tanaka, W.; Sada, K.; Kubota, R.; Aoyama, T.; Urayama, K.; Hamachi, I. Phototriggered Spatially Controlled Out-of-Equilibrium Patterns of Peptide Nanofibers in a Self-Sorting Double Network Hydrogel. *J. Am. Chem. Soc.* **2021**, *143* (46), 19532–19541. <https://doi.org/10.1021/jacs.1c09172>.
- (35) Chen, C.; Valera, J. S.; Adachi, T. B. M.; Hermans, T. M. Efficient Photoredox Cycles to Control Peryleneimide Self-Assembly\*\*. *Chemistry – A European Journal* **2023**, *29* (1), e202202849. <https://doi.org/10.1002/chem.202202849>.
- (36) Deng, J.; Bezold, D.; Jessen, H. J.; Walther, A. Multiple Light Control Mechanisms in ATP-Fueled Non-equilibrium DNA Systems. *Angewandte Chemie* **2020**, *132* (29), 12182–12190. <https://doi.org/10.1002/ange.202003102>.
- (37) Xu, F.; Crespi, S.; Pacella, G.; Fu, Y.; Stuart, M. C. A.; Zhang, Q.; Portale, G.; Feringa, B. L. Dynamic Control of a Multistate Chiral Supramolecular Polymer in Water. *J. Am. Chem. Soc.* **2022**, *144* (13), 6019–6027. <https://doi.org/10.1021/jacs.2c01063>.
- (38) Singh, N.; Lainer, B.; Formon, G. J. M.; De Piccoli, S.; Hermans, T. M. Re-Programming Hydrogel Properties Using a Fuel-Driven Reaction Cycle. *Journal of the American Chemical Society* **2020**, *142* (9), 4083–4087. <https://doi.org/10.1021/jacs.9b11503>.
- (39) Singh, N.; Lopez-Acosta, A.; Formon, G. J. M.; Hermans, T. M. Chemically Fueled Self-Sorted Hydrogels. *J. Am. Chem. Soc.* **2022**, *144* (1), 410–415. <https://doi.org/10.1021/jacs.1c10282>.
- (40) Hermans, T.; Singh, N. Chemically Fueled Autonomous Sol→Gel→Sol→Gel→Sol Transitions. *Angewandte Chemie International Edition* **2023**, *62* (23), e202301529. <https://doi.org/10.1002/anie.202301529>.
- (41) Cibulka, R.; Vasold, R.; König, B. Catalytic Photooxidation of 4-Methoxybenzyl Alcohol with a Flavin–Zinc(II)–Cyclen Complex. *Chemistry – A European Journal* **2004**, *10* (24), 6223–6231. <https://doi.org/10.1002/chem.200400232>.
- (42) Schmäderer, H.; Hilgers, P.; Lechner, R.; König, B. Photooxidation of Benzyl Alcohols with Immobilized Flavins. *Advanced Synthesis & Catalysis* **2009**, *351* (1–2), 163–174. <https://doi.org/10.1002/adsc.200800576>.
- (43) Dađová, J.; Kümmel, S.; Feldmeier, C.; Cibulková, J.; Pažout, R.; Maixner, J.; Gschwind, R. M.; König, B.; Cibulka, R. Aggregation Effects in Visible-Light Flavin Photocatalysts: Synthesis, Structure, and Catalytic Activity of 10-Arylflavins. *Chemistry – A European Journal* **2013**, *19* (3), 1066–1075. <https://doi.org/10.1002/chem.201202488>.
- (44) Leiva, C.; Lo, H. C.; Fish, R. H. Aqueous Organometallic Chemistry. 3. Catalytic Hydride Transfer Reactions with Ketones and Aldehydes Using [Cp\*Rh(Bpy)(H<sub>2</sub>O)](OTf)<sub>2</sub> as the Precatalyst and Sodium Formate as the Hydride Source: Kinetic and Activation Parameters, and the Significance of Steric and Electronic Effects. *J. Organometallic Chem.* **2010**, *695* (2), 145–150.
- (45) Givens, R. S.; Rubina, M.; Wirz, J. Applications of P-Hydroxyphenacyl (pHP) and Coumarin-4-Ylmethyl Photoremovable Protecting Groups. *Photochem. Photobiol. Sci.* **2012**, *11* (3), 472–488. <https://doi.org/10.1039/C2PP05399C>.
- (46) Lo, H. C.; Leiva, C.; Buriez, O.; Kerr, J. B.; Olmstead, M. M.; Fish, R. H. Bioorganometallic Chemistry. 13. Regioselective Reduction of NAD<sup>+</sup> Models, 1-Benzylnicotinamide Triflate and β-Nicotinamide Ribose-5'-Methyl Phosphate, with in Situ Generated [Cp\*Rh(Bpy)H]<sup>+</sup>: Structure–Activity Relationships, Kinetics, and Mechanistic Aspects in the Formation of the 1,4-NADH Derivatives. *Inorg. Chem.* **2001**, *40* (26), 6705–6716. <https://doi.org/10.1021/ic010562z>.
- (47) Fan, B.; Men, Y.; van Rossum, S. A. P.; Li, G.; Eelkema, R. A Fuel-Driven Chemical Reaction Network Based on Conjugate Addition and Elimination Chemistry. *ChemSystemsChem* **2020**, *2* (1), e1900028. <https://doi.org/10.1002/syst.201900028>.

- (48) Speckmeier, E.; Zeitler, K. Desyl and Phenacyl as Versatile, Photocatalytically Cleavable Protecting Groups: A Classic Approach in a Different (Visible) Light. *ACS Catal.* **2017**, *7* (10), 6821–6826. <https://doi.org/10.1021/acscatal.7b02117>.
- (49) Gelebart, A. H.; Jan Mulder, D.; Varga, M.; Konya, A.; Vantomme, G.; Meijer, E. W.; Selinger, R. L. B.; Broer, D. J. Making Waves in a Photoactive Polymer Film. *Nature* **2017**, *546* (7660), 632–636. <https://doi.org/10.1038/nature22987>.
- (50) Li, C.; Iscen, A.; Sai, H.; Sato, K.; Sather, N. A.; Chin, S. M.; Álvarez, Z.; Palmer, L. C.; Schatz, G. C.; Stupp, S. I. Supramolecular–Covalent Hybrid Polymers for Light-Activated Mechanical Actuation. *Nature Materials* **2020**, *19* (8), 900–909. <https://doi.org/10.1038/s41563-020-0707-7>.